Structural Engineering and Mechanics, *Vol. 63, No. 2 (2017) 181-193*
DOI: https://doi.org/10.12989/sem.2017.63.2.181

Parameters identification of fractional models of viscoelastic dampers and fluids

Roman Lewandowski*[1], Mieczysław Słowik[2] and Maciej Przychodzki[1]

[1]*Institute of Structural Engineering, Poznan University of Technology, ul. Piotrowo 5, 60-965 Poznan, Poland*
[2]*Institute of Civil Engineering, Poznan University of Technology, ul. Piotrowo 5, 60-965 Poznan, Poland*

(Received July 21, 2016, Revised December 10, 2016, Accepted February 24, 2017)

Abstract. An identification method for determination of the parameters of the rheological models of dampers made of viscoelastic material is presented. The models have two, three or four parameters and the model equations of motion contain derivatives of the fractional order. The results of dynamical experiments are approximated using the trigonometric function in the first part of the procedure while the model parameters are determined as the solution to an appropriately defined optimization problem. The particle swarm optimization method is used to solve the optimization problem. The validity and effectiveness of the suggested identification method have been tested using artificial data and a set of real experimental data describing the dynamic behavior of damper and a fluid frequently used in dampers. The influence of a range of excitation frequencies used in experiments on results of identification is also discussed.

Keywords: viscoelastic dampers and fluids, fractional rheological models, identification of parameter

1. Introduction

Viscoelastic (VE) dampers have often been used in civil engineering to reduce excessive oscillations of building structures due to earthquakes and strong winds. A number of applications of VE dampers in civil engineering are listed in the book by Christopoulos and Filiatrault (2006). Moreover, VE dampers are also used to reduce the vibrations of aircrafts, aerospace and machine structures. The VE dampers could be divided into fluid and solid VE dampers. Silicone oil is used to build the fluid dampers while the solid dampers are made of copolymers or glassy substances.

A comparative study on parameter identification for fluid viscous dampers was presented by Greco *et al.* (2014). The properties and rheological models of fluids dampers are identified on the basis of results of experiments which are laborious and expensive. Moreover, such experiments can usually be conducted only for low excitation frequencies. Some attempts of numerical modelling of the flow of fluids in damper cylinder can be found in papers by Hou (2008) and by Frings and De La Llero (2011). The results of such types of calculation can be used in the identification procedure for damper model parameters and are able to significantly reduce the number of the required physical experiments. Of course, this approach requires the knowledge of the properties of the fluid used in the damper. However, experiments with the above-mentioned fluids can be performed for a wide range of excitation frequencies and with control of temperature during the experiments, using rheometers. The fluids used in dampers are usually highly viscous and their constitutive equations often contain fractional derivatives (see, for example, papers by Tong and Liu 2005 and by Yang *et al.* 2010).

A good mathematical model of dampers is required for the dynamic analysis of structures with VE dampers embedded in them. The rheological properties of the viscoelastic material dampers are made of and some of the geometric parameters of dampers are the main factors which determine the dampers dynamic behaviour. In the case of fluid dampers, the rheological model of a highly viscous fluid used in the damper is also very important. The complex modulus concept is widely used to describe the dynamic characteristics of VE materials (see, for example the book by Jones 2001). Both terms of the complex modulus of damping materials, i.e., the storage modulus and the loss modulus, depend on the frequency of oscillations, and temperature.

In the past, several rheological models were proposed to describe the dynamic behaviour of VE materials and dampers. Both the classical and the so-called fractional-derivative models of dampers and VE materials are available. Descriptions of these models are given, among others, in papers by Bagley and Torvik (1989), Park (2001), Makris and Constantinou (1991), Pritz (1996, 2003), Aprile *et al.* (1997), Indesman *et al.* (2001), Lewandowski *et al.* (2012) and Xu and Jiang (2016).

The classical rheological models consisting of springs and dashpots are used by Park (2001), Singh and Moreschi (2002), Shukla and Datta (1999) and by Palmeri *et al.* (2003) to describe the rheological properties of VE dampers. Due to their simplicity, the simple models, such as the Kelvin model or the Maxwell model, are used very often to describe the dynamic behaviour of VE dampers installed on various types of civil engineering structures.

*Corresponding author, Professor
E-mail: roman.lewandowski@put.poznan.pl

ISSN: 1225-4568 (Print), 1598-6217 (Online)

For example, the Kelvin model is used in papers by Singh and Moreschi (2002), Shukla and Datta (1999), Matsagar and Jangid (2005), Lee *et al.* (2004) and by Park *et al.* (2004), while the Maxwell model is used in papers by Singh *et al.* (2002, 2003), Shukla and Datta (1999) and Hatada *et al.* (2000). However, these simple models are not able to correctly describe the dynamic behaviour of VE materials or dampers. A correct description of the VE dampers requires rheological models which are built of a set of appropriately connected springs and dashpots. In this case, the dynamic behaviour of a single damper is described by a set of differential equations (see papers by Park 2001, Palmeri *et al.* 2003 and by Singh *et al.* 2009), which considerably complicates the dynamic analysis of structures with dampers.

Rheological models of VE dampers and fluids with fractional derivatives, which will be referred to in this paper as the fractional rheological models, have received considerable attention. The reason is their ability to correctly describe the behaviour of VE dampers in a wide range of excitation frequencies and using a smaller number of model elements (and parameters), compared with the classic rheological models. A single equation is enough to describe the VE damper dynamics, which is an important advantage of the discussed models. However, in this case, the VE damper equation of motion is the fractional differential equation. The fractional rheological models have been used in modelling the rheological behaviour of VE materials (see papers by Bagley and Torvik 1989, Enelund and Olsson 1999 and by Fenander 1996) and dampers (see papers by Makris and Constantinou 1991, Aprile *et al.* 1997 and by Lewandowski and Pawlak 2011). A very simple model of viscoelastic materials comprising only one springpot elements was proposed by Di Paola *et al.* (2011) and used in papers by Pirrotta *et al.* (2015) and by Bucher and Pirrotta (2015) in the static and dynamic analysis of beams and structures made of viscoelastic materials.

The dynamic analyses of frame structures with dampers modelled using the fractional rheological models are also presented in papers by Chang and Singh (2002), Lewandowski and Pawlak (2011) and by Tsai *et al.* (2002) where either the fractional Maxwell model or the fractional Kelvin model are used to describe the dampers dynamic behaviour. Moreover, in paper by Okada *et al.* (2006) the rational polynomial approximation modelling is used for analysis of structures with VE dampers. The fractional derivative model of damping was applied also to description of dynamic behaviour of viscoelastic beams (see papers by Galucio *et al.* (2004), Cortes and Elejabarrieta (2007). The finite element formulation of fractional viscoelastic constitutive equations is presented by Schmidt and Gaul (2002).

An important problem to which the paper relates is the estimation of model parameters using experimental data. The process of parameter identification is an inverse problem which can be ill conditioned (see, for example papers by Hansen 2007 and Gerlach and Matzenmiller 2005) because of noises existing in the experimental data. Recently, the identification procedures for the three parameters fractional Kelvin-Voigt model and the fractional Maxwell model are proposed by Lewandowski and Chorążyczewski (2010). The problem of parameters identification of rheological models with fractional derivatives is also discussed by Makris and Constantinou (1991), Pritz (1996, 2003), Gusella and Terenzi (1997), Aprile *et al.* (1997) and by Gupta *et al.* (1996). Static data were used in paper by Welch *et al.* (1999) to determine the parameters of new fractional calculus-based constitutive equations of viscoelastic materials. A procedure for the calculation of the parameters of two classic models: a Kelvin chain and a Maxwell ladder, is presented by Chang and Singh (2009). Moreover, for the generalized fractional Zener model, Fan *et al*. (2015) used the Bayesian method for estimating the parameters of the considered model.

A new method for identification of the parameters of the fractional model of VE dampers and fluids with different numbers of parameters is presented in this paper. The results of real dynamic tests are used to identify the parameters of a damper model. The identification procedure comprises two main steps. Experimental results are approximated by a simple harmonic function in the time domain in the first step while model parameters are determined in the second stage of the identification procedure. The particle swarm optimization method is used in the second step of the identification procedure. The validity, accuracy and effectiveness of the procedures have been tested using both artificial and real experimental data. The method is rather general because it is possible to identify the parameters of different rheological models in a unified way.

The paper is organized as follows: In Section 2, the equation of motion of the considered rheological models and the steady state solution to this equation is derived. A description of the identification procedure is given in Section 3. In Section 4, details of the applied particle swarm optimization method are described. Various examples are studied in Section 5 while the concluding remarks are presented in Section 6.

2. Description of rheological models and their steady state vibration

2.1 Rheological models of VE dampers

Rheological models with three or four parameters are considered. First of all, we introduce a fractional element called the springpot, shown separately in Fig. 1 and as the rhombus in the below-presented figures. The springpot element satisfies the following constitutive equation

$$u(t) = c\, D_t^{\alpha} q(t) \tag{1}$$

where c and α, $0 < \alpha \le 1$, are the springpot parameters and $D_t^{\alpha} q(t)$ is the fractional derivative of the order α of consecutive function, here $q(t)$, with respect to time t. There are a few definitions of fractional derivatives which coincide under certain conditions. Here, symbols such as $D_t^{\alpha} q(t)$ denote the Riemann-Liouville fractional

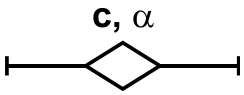

Fig. 1 The springpot element

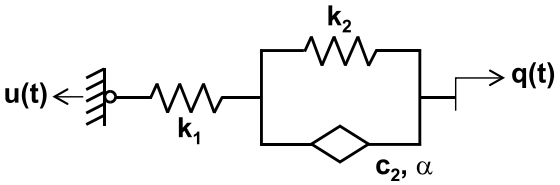

Fig. 2 The Kelvin type four-parameter model of VE dampers

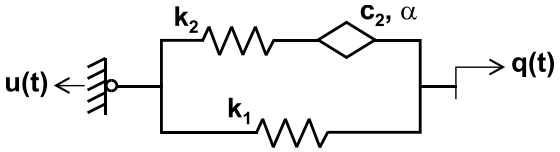

Fig. 3 The Maxwell type four-parameter model of VE dampers

derivatives with the lower limit at $-\infty$. Some valuable information about fractional calculus can be found in the book by Podlubny (1999). The considered fractional derivative of function $x(t)$ is defined as

$$D^{\alpha}x(t)=\frac{1}{\Gamma(1-\alpha)}\frac{d}{dt}\int_{-\infty}^{t}\frac{x(\tau)}{(t-\tau)^{\alpha}}d\tau \tag{2}$$

where Γ is the gamma function. The springpot element is also known as the Scott-Blair element. The considered element can be understood as an interpolation between the spring element (α=0) and the dashpot element (α=1).

The first model, which will be called the Kelvin type four-parameter model, is a combination of the spring element and the fractional Kelvin element (see Fig. 2). The constitutive equations are

$$u(t)=k_1 q_d(t) \tag{3}$$

for the spring element and

$$u(t)=k_2(q(t)-q_d(t))+c_2 D_t^{\alpha}(q(t)-q_d(t)) \tag{4}$$

for the fractional Kelvin element where $q_d(t)$ is the so-called internal variable which can be understood here as the relative displacement of the spring element.

After eliminating the internal variable from relationships (3) and (4), the following equation of motion of the first rheological model is obtained

$$u(t)+\tau^{\alpha}D_t^{\alpha}u(t)=k_0 q(t)+k_{\infty}\tau^{\alpha}D_t^{\alpha}q(t) \tag{5}$$

where

$$k_0=k_1k_2/(k_1+k_2),\quad k_{\infty}=k_1,\quad \tau^{\alpha}=c_2/(k_1+k_2) \tag{6}$$

The second model, which will be called the Maxwell type four-parameters model, consists of the spring element and the fractional Maxwell element connected in parallel (see Fig. 3). The behaviour of these elements is described by the following equations

$$u(t)=u_1(t)+u_2(t)\quad,\qquad u_1(t)=k_1 q(t) \tag{7}$$

$$u_2(t)+\frac{c_2}{k_2}D_t^{\alpha}u_2(t)=c_2 D_t^{\alpha}q(t) \tag{8}$$

After eliminating $u_1(t)$ and $u_2(t)$ from the above relationships again Eq. (5) is obtained, but now

$$k_0=k_1,\quad k_{\infty}=k_1+k_2,\quad \tau^{\alpha}=c_2/k_2 \tag{9}$$

In conclusion, the dynamic behaviour of both of the considered models is described with the help of Eq. (5).

If the damper is harmonically excited, i.e., $q(t)=q_0\exp(i\lambda t)$, where $i^2=-1$ is the imaginary unit and λ is the excitation frequency, the damper force in the case of steady state vibration can be described as

$$u(t)=u_0\exp(i\lambda t) \tag{10}$$

After introducing the above relationships into Eq. (5) and taking into account that $D_t^{\alpha}\exp(i\lambda t)=(i\lambda)^{\alpha}\exp(i\lambda t)$ we obtain

$$u_0=\frac{k_0+k_{\infty}(i\lambda\tau)^{\alpha}}{1+(i\lambda\tau)^{\alpha}}q_0 \tag{11}$$

Very often the damper's complex stiffness is introduced. This quantity is defined as

$$K(\lambda)=K'(\lambda)+i\,K''(\lambda)=K'(\lambda)\left[1+i\,\eta(\lambda)\right] \tag{12}$$

where $K'(\lambda)$ is the storage modulus, $K''(\lambda)$ is the loss modulus and $\eta(\lambda)=K''(\lambda)/K'(\lambda)$ is the loss factor. After introducing the following formula $i^{\alpha}=\cos(\alpha\pi/2)+i\sin(\alpha\pi/2)$, we can write

$$K'(\lambda)=\frac{k_0+(k_0+k_{\infty})(\tau\lambda)^{\alpha}\cos(\alpha\pi/2)+k_{\infty}(\tau\lambda)^{2\alpha}}{1+2(\tau\lambda)^{\alpha}\cos(\alpha\pi/2)+(\tau\lambda)^{2\alpha}} \tag{13}$$

$$K''(\lambda)=\frac{(k_{\infty}-k_0)(\tau\lambda)^{\alpha}\sin(\alpha\pi/2)}{1+2(\tau\lambda)^{\alpha}\cos(\alpha\pi/2)+(\tau\lambda)^{2\alpha}} \tag{14}$$

$$\eta(\lambda)=\frac{(k_{\infty}-k_0)(\tau\lambda)^{\alpha}\sin(\alpha\pi/2)}{k_0+(k_0+k_{\infty})(\tau\lambda)^{\alpha}\cos(\alpha\pi/2)+k_{\infty}(\tau\lambda)^{2\alpha}} \tag{15}$$

Based on the results presented by Lion (2001), it can be easily demonstrated that this model fulfils the second law of thermodynamics for $0\le\alpha\le1$, $\tau>0$ and $k_{\infty}>k_0>0$.

If the damper's steady state vibration is analysed using real numbers then

$$\begin{aligned}u(t)&=u_c\cos\lambda t+u_s\sin\lambda t,\\ q(t)&=q_c\cos\lambda t+q_s\sin\lambda t\end{aligned} \tag{16}$$

and the parameters u_c, u_s, q_c and q_s fulfil the following

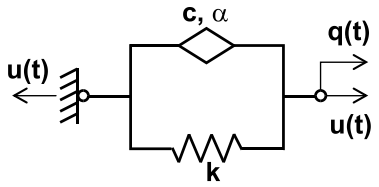

Fig. 4 The three-parameter Kelvin model of VE dampers

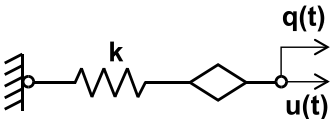

Fig. 5 The three-parameter Maxwell model of VE dampers

relationships

$$u_c = z_1(\lambda)q_c + z_2(\lambda)q_s, \quad u_s = -z_2(\lambda)q_c + z_1(\lambda)q_s \tag{17}$$

where

$$z_1(\lambda) \equiv K'(\lambda), \qquad z_2(\lambda) \equiv K''(\lambda) \tag{18}$$

and we take into account that

$$\begin{aligned} D_t^\alpha \cos\lambda t &= \lambda^\alpha \cos(\lambda t + \alpha\pi/2) \\ D_t^\alpha \sin\lambda t &= \lambda^\alpha \sin(\lambda t + \alpha\pi/2) \end{aligned} \tag{19}$$

Moreover, two fractional rheological models with three parameters, i.e., the fractional Kelvin model and the fractional Maxwell model shown in Figs. 4 and 5, respectively, are considered.

The equation of motion of the three-parameter models is

$$u(t) = kq(t) + k\tau^\alpha D_t^\alpha q(t) \tag{20}$$

for the Kelvin model and

$$u_2(t) + \tau^\alpha D_t^\alpha u_2(t) = k\tau^\alpha D_t^\alpha q(t) \tag{21}$$

for the Maxwell model, where $\tau^\alpha = c/k$.

The storage modulus and the loss modulus could be determined from the following formulas

$$\begin{aligned} K'(\lambda) &= k[1 + (\tau\lambda)^\alpha \cos(\alpha\pi/2)] \\ K'' &= k(\tau\lambda)^\alpha \sin(\alpha\pi/2) \end{aligned} \tag{22}$$

for the Kelvin model and

$$K'(\lambda) = k(\tau\lambda)^\alpha \frac{(\tau\lambda)^\alpha + \cos(\alpha\pi/2)}{1 + (\tau\lambda)^{2\alpha} + 2(\tau\lambda)^\alpha \cos(\alpha\pi/2)} \tag{23}$$

$$K''(\lambda) = k(\tau\lambda)^\alpha \frac{\sin(\alpha\pi/2)}{1 + (\tau\lambda)^{2\alpha} + 2(\tau\lambda)^\alpha \cos(\alpha\pi/2)} \tag{24}$$

for the Maxwell model, respectively.

The three-parameter models fulfill the second law of thermodynamics for $0 \le \alpha \le 1$, $\tau > 0$ and $k > 0$. Moreover, the three-parameter fractional models fulfill also Eq. (17).

In the case of dampers, the model proposed by Di Paola (2011) is described by Eq. (1) while the storage and loss modulus and the loss factor are given by

$$K'(\lambda) = c\lambda^\alpha \cos(\alpha\pi/2), \quad K'' = c\lambda^\alpha \sin(\alpha\pi/2) \tag{25}$$

$$\eta = K''(\lambda)/K'(\lambda) = tg(\alpha\pi/2) \tag{26}$$

In contrast to the previous models, the loss factor of the considered model is independent of excitation frequency.

2.2 Rheological models of highly viscous fluids

The most popular models of highly viscous fluids are the fractional model and the fractional Oldroyd-B model. In the case of one-dimensional flow, the constitutive equation of Maxwell fluids is (see, for example, papers by Yin and Zhu 2006 and by Hayat *et al.* 2004)

$$\sigma(t) + \tau^\alpha D_t^\alpha \sigma(t) = E\tau^\beta D_t^\beta \varepsilon(t) \tag{27}$$

where $\sigma(t)$ is the shear stress, $\varepsilon(t)$ is the shear strain, E is the shear modulus, $\tau^\alpha = \eta/E$, η is the viscosity constant. Moreover, α and β are the fractional parameters fulfilling the restriction $0 < \alpha \le \beta \le 1$. Often $\beta = 1$ and here, it is assumed that $\alpha = \beta$. It is to be noted that the coefficients η has an anomalous dimension which depends on the value of α. The unit of η is [Pa·s$^\alpha$].

As presented by Khan *et al.* (2010), the constitutive equation for the Oldroyd-B fluids could be written (using a little bit different notations) in the following form

$$\sigma(t) + \tau^\alpha D_t^\alpha \sigma(t) = E_0\varepsilon(t) + \tau^\alpha E_\infty D_t^\alpha \varepsilon(t) \tag{28}$$

where E_0 and E_∞ are the non-relaxed and relaxed shear modulus, respectively.

A formal similarity between Eqs. (27), (28) and Eqs. (21), (5) and all the resulting equations is obvious. In particular, the storage modulus and the loss modulus are given by

$$E'(\lambda) = E(\tau\lambda)^\alpha \frac{(\tau\lambda)^\alpha + \cos(\alpha\pi/2)}{1 + 2(\tau\lambda)^\alpha \cos(\alpha\pi/2) + (\tau\lambda)^{2\alpha}} \tag{29}$$

$$E''(\lambda) = E(\tau\lambda)^\alpha \frac{\sin(\alpha\pi/2)}{1 + 2(\tau\lambda)^\alpha \cos(\alpha\pi/2) + (\tau\lambda)^{2\alpha}} \tag{30}$$

for the Maxwell fluids and

$$E'(\lambda) = \frac{E_0 + (E_0 + E_\infty)(\tau\lambda)^\alpha \cos(\alpha\pi/2) + E_\infty(\tau\lambda)^{2\alpha}}{1 + 2(\tau\lambda)^\alpha \cos(\alpha\pi/2) + (\tau\lambda)^{2\alpha}} \tag{31}$$

$$E''(\lambda) = \frac{(E_\infty - E_0)(\tau\lambda)^\alpha \sin(\alpha\pi/2)}{1 + 2(\tau\lambda)^\alpha \cos(\alpha\pi/2) + (\tau\lambda)^{2\alpha}} \tag{32}$$

for the Oldroyd-B fluids.

In this paper, a family of fractional rheological models are considered in order to describe the behavior of high-viscosity fluids. It contains the three-parameter Kelvin model (see Fig. 6(a)), the three-parameter Maxwell model

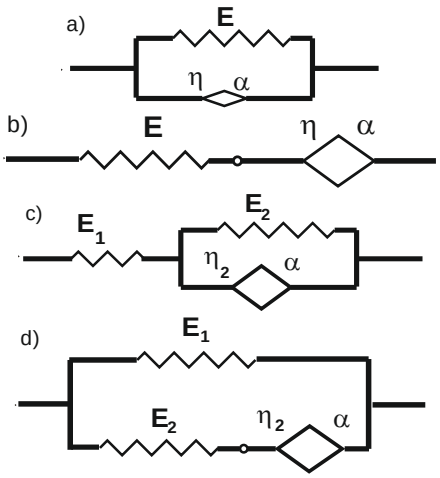

Fig. 6 Schematic view of fractional rheological models, a) three-parameter Kelvin model, b) three-parameter Maxwell model, c) fourth-parameter standard model, d) fourth-parameter Zener model

(Fig. 6(b)) and two versions of the four-parameter model, i.e., the standard model (Fig. 6(c)) and the Zener model (Fig. 6(d)).

The equation of motion of the three-parameter Kelvin model is given by

$$\sigma(t) = E\varepsilon(t) + E\tau^{\alpha} D_t^{\alpha}\varepsilon(t) \tag{33}$$

where $\tau^{\alpha}=\eta/E$ (compare Fig. 6(a)), while the equation of motion of the three-parameter Maxwell model is described by Eq. (27) for $\alpha=\beta$.

The behavior of both versions of the four-parameter model is governed by Eq. (28) where now

$$E_0 = E_1E_2/(E_1+E_2), \qquad E_{\infty} = E_1, \qquad \tau^{\alpha} = \eta_2/(E_1+E_2) \tag{34}$$

for the standard model and

$$E_0 = E_1, \qquad E_{\infty} = E_1+E_2, \qquad \tau^{\alpha} = \eta_2/E_2 \tag{35}$$

for the Zener model. Meaning of symbols E_1, E_2 and η_2 are obvious from Fig. 6.

3. Description of identification method

In this Section we assume that, during the experimental tests, two output functions $u_e(t)$ (function of force in a time domain) and $q_e(t)$ (function of displacement in a time domain) were obtained. During experiments, the damper is several times harmonically excited and in each case the excitation frequency, denoted here as λ_i, (i=1,2,…,n), is different. The steady state response of the damper is measured, which means that the experimental damper displacements $q_{ei}(t)$ and the experimental damper forces $u_{ei}(t)$ are known for each excitation frequency λ_i. It is assumed that all experiments are performed at a constant ambient temperature and changes of damper's temperature during the test are negligible.

The identification procedure consists of two main steps. In the first step the experimental results are approximated by a simple harmonic function in the time domain while the model parameters are determined in the second stage of the identification procedure.

In the first step, experimentally measured displacements $q_e(t)$ of the damper are approximated using the function

$$\tilde{q}(t) = \tilde{q}_c\cos\lambda t + \tilde{q}_s\sin\lambda t \tag{36}$$

The least-square method is used to determine parameters $\tilde{q}_c$ and $\tilde{q}_s$ of function (33). This method requires minimization of the following functional

$$J_1(\tilde{q}_c,\tilde{q}_s) = \frac{1}{t_2-t_1}\int_{t_1}^{t_2}\left[q_e(t)-\tilde{q}(t)\right]^2 dt \tag{37}$$

where the symbols t_1 and t_2 denote the beginning and the end of the time range in which the damper's displacements were measured. Part of the measuring results relating to a steady state vibration is used as data in this step. From the stationary conditions of the functional (37), the following system of equations is obtained

$$I_{cc}\tilde{q}_c + I_{sc}\tilde{q}_s = I_{cq}\ , \qquad I_{sc}\tilde{q}_c + I_{ss}\tilde{q}_s = I_{sq} \tag{38}$$

from which the parameters $\tilde{q}_c$ and $\tilde{q}_s$ are obtained and where

$$I_{cc} = \int_{t_1}^{t_2}\cos^2\lambda t dt, \qquad I_{ss} = \int_{t_1}^{t_2}\sin^2\lambda t dt$$
$$I_{cs} = I_{sc} = \int_{t_1}^{t_2}\sin\lambda t\cos\lambda t dt \tag{39}$$

$$I_{cq} = \int_{t_1}^{t_2} q_e(t)\cos\lambda\, t\, dt, \qquad I_{sq} = \int_{t_1}^{t_2} q_e(t)\sin\lambda\, t\, dt \tag{40}$$

Similarly, the experimentally measured dampers force $u_e(t)$ is approximated by

$$\tilde{u}(t) = \tilde{u}_c\cos\lambda t + \tilde{u}_s\sin\lambda t \tag{41}$$

Proceeding to a description of the second step of the identification method, it is assumed that a set of results of the above-described first step of the procedure given by $\tilde{u}_{ci}$, $\tilde{u}_{si}$, $\tilde{q}_{ci}$ and $\tilde{q}_{si}$ and relating to the different excitation frequencies λ_i $(i=1,2,...,n)$ is known. If the considered rheological model is able to correctly simulate the VE damper behaviour then the relationships (17) must approximately be fulfilled by the above-mentioned results of the first step identification procedure, i.e.

$$\tilde{u}_{ci} = \tilde{z}_{1i}\tilde{q}_{ci} + \tilde{z}_{2i}\tilde{q}_{si}\ , \qquad \tilde{u}_{si} = -\tilde{z}_{2i}\tilde{q}_{ci} + \tilde{z}_{1i}\tilde{q}_{si}\ , \tag{42}$$

where i=1,2,…,n.

Solving Eq. (15) with respect to $\tilde{z}_{1i}$ and $\tilde{z}_{2i}$ the

following is obtained

$$\tilde{z}_{1i} = \frac{\tilde{u}_{ci}\tilde{q}_{ci} + \tilde{u}_{si}\tilde{q}_{si}}{\tilde{q}_{ci}^2 + \tilde{q}_{si}^2} \quad , \qquad \tilde{z}_{2i} = \frac{\tilde{u}_{ci}\tilde{q}_{si} - \tilde{u}_{si}\tilde{q}_{ci}}{\tilde{q}_{ci}^2 + \tilde{q}_{si}^2} \tag{43}$$

Results of experiments are often presented in the form of curves or tables where relationships $K'(\lambda)$, $K''(\lambda)$ are given. In this case, Eqs. (42) or (43) could be used to determine the parameters $\tilde{u}_{ci}$ and $\tilde{u}_{si}$ after choosing the values of parameters $\tilde{q}_{ci}$ and $\tilde{q}_{si}$. This procedure assumes that rheological models are described with the help of linear differential equations (with the ordinary as well as the fractional derivatives).

If the rheological model perfectly fits with the experimental data, then $z_{1i} - \tilde{z}_{1i} = 0$ and $z_{2i} - \tilde{z}_{2i} = 0$ for i=1,2,…,n, where $z_{1i} = z_1(\lambda_i)$, $z_{2i} = z_2(\lambda_i)$ are calculated using formulae for $K'(\lambda)$ and $K''(\lambda)$ or for E'(λ) and $E''(\lambda)$, derived above for the respective models. In practice, some differences usually do exist and parameters of the rheological model are determined as the solution to an appropriately defined optimization problem.

In the paper the above-mentioned optimization problem is formulated as follows:

Find the values of parameters of the considered model (i.e., k_0, k_∞, τ and α for the four-parameter model and k, τ and α for the three-parameter models) which minimize the functional

$$J = \sum_{i=1}^{n} \left[(z_{1i} - \tilde{z}_{1i})^2 + (z_{2i} - \tilde{z}_{2i})^2 \right] \tag{44}$$

and fulfil the following constraints

$$0 < \alpha \le 1, \qquad \tau > 0, \qquad k_\infty > k_0 > 0 \quad , \tag{45}$$

$$0 < \alpha \le 1, \qquad \tau > 0, \qquad k > 0 \quad , \tag{46}$$

$$0 < \alpha \le 1, \qquad c > 0 \tag{47}$$

for the four-parameter models, for the three-parameter models and for the two-parameter model, respectively.

The above optimization problem is solved with the help of the particle swarm optimization method described, for example in paper by Perez and Behdinan (2007), and, briefly, in the next Section. The fractional version of the particle swarm optimization is described in the very recent book by Couceiro and Ghamisi (2016).

4. Description of the adopted version of the particle swarm optimization method

The particle swarm optimization (PSO), developed by Kennedy and Eberhardt (1995), is based on the observation of the social behavior of animals, such as bird flocking, fish schooling and the swarm theory. Bird flocks, fish schools, and other populations' swarms are capable of finding optimum locations upon relying on their distributed intelligence. PSO has memory. The knowledge of good solutions is retained by all particles. In PSO, there exists a constructive cooperation between the particles that share information.

PSO is an evolutionary computation technique through individual improvement in addition to population cooperation and competition. In PSO, multiple candidate solutions coexist and collaborate simultaneously. Each solution (called a particle) moves in the exploration space of the optimization problem and searching the optimal position. As time passes through its quest, a particle adapts to adjust its position according to its own 'experience' as well as the experiences of its neighboring particles. With tracking and memorizing the best position encountered, the experiences of particles are accumulated as exploration proceeds. Thus, PSO possesses memory, i.e., every particle remembers the best position it reached in the past. At the same time, PSO combines the local search scheme through self-experience with the global search scheme through neighboring experience so that the best solution is obtained at the end.

Each particle is characterized by the vector of particle position and the vector of particle velocity. The position vector $\mathbf{p}_j$ and the velocity vector $\mathbf{v}_j$ of the j-th particle each contain the parameters of the considered fractional rheological models, i.e.

$$\mathbf{p}_j = col(p_{1,j} = k_0, p_{2,j} = k_\infty, p_{3,j} = \tau, p_{4,j} = \alpha) \tag{48}$$

$$\mathbf{p}_j = col(p_{1,j} = k, \ p_{2,j} = \tau, \ p_{3,j} = \alpha) \tag{49}$$

for the four- and three-parameters models, respectively. The search for optimal solutions is performed by updating the subsequent positions of particles. Moreover, each particle keeps record of its best fitness achieved so far as the vector $\mathbf{b}_j$ and the best fitness and corresponding solution achieved in the particle's neighborhood as the vector $\mathbf{g}_j$. It was shown that using global neighborhood (all particles are fully aware of other particles' fitness) minimizes the median number of iterations needed to converge. On the other hand, the neighborhood of size two gives the highest resistance to local minima.

At each time instances i of the PSO, the velocities of the particles are changed (accelerated) towards the $\mathbf{b}_j(i)$ and the $\mathbf{g}_j(i)$ and the particles are moved to new positions according to the following formulas taken from the paper by Wilke *et al.* (2007)

$$\mathbf{v}_j(i+1) = w(i)\mathbf{v}_j(i) + \frac{c_1}{\Delta t}\mathbf{R}_1(i)\left[\mathbf{b}_j(i) - \mathbf{p}_j(i)\right] + \frac{c_2}{\Delta t}\mathbf{R}_2(i)\left[\mathbf{g}_j(i) - \mathbf{p}_j(i)\right]/\Delta t \tag{50}$$

$$\mathbf{p}_j(i+1) = \mathbf{p}_j(i) + \mathbf{v}_j(i+1)\Delta t \tag{51}$$

where Δt=1, $\mathbf{R}_1(i)$, $\mathbf{R}_2(i)$ are the diagonal matrices of independent random numbers uniformly distributed in the range [0, 1]; $\mathbf{v}_j(i)$ and $\mathbf{p}_j(i)$ are the velocity and the position vectors at the i-th instance of time, respectively; $w(i)$ $w(i)$ is the inertia factor providing balance between exploration and exploitation, c_1 is the individuality constant, and c_2 is the

sociality constant. To speed up convergence, the inertia weight was linearly reduced from $w_{\max}$ to $w_{\min}$, i.e.

$$w(i+1) = w_{\max} - (w_{\max} - w_{\min})\, i / i_{\max} \tag{52}$$

Where $i_{\max}$ is the maximal number of time instances.

Zero vectors are chosen as the initial values of velocity vectors $\mathbf{v}_j(0)$. The initial values of parameters τ and α, i.e., elements vectors $\mathbf{p}_j(0)$, are chosen as random, uniformly distributed numbers taken from the range [0, 1]. The initial values of stiffness parameters k_0 and k_∞ or k are chosen as the random numbers uniformly distributed in the range [0, 1] multiplied by some constant $\bar{k}$, which means that, for example, the initial values of k_0 are calculated from the formula $k_0 = r\,\bar{k}$. The values of $\bar{k}$ are chosen of the order of the expected values of stiffness parameters k_∞ or k. The above choices assure all assumed initial approximations of dampers parameters, i.e., vectors $\mathbf{p}_j(0)$ and $\mathbf{v}_j(0)$ fulfil the optimization constraints (45), (46) or (47).

An important part of the PSO algorithm is the way of handling the constraints, introduced by the considered optimization problem. The value of each component in $\mathbf{v}_j(i)$ is clamped to the range $[v_{\min}, v_{\max}]$ to control the excessive roaming of particles outside the search space. The values $v_{\min}$=-0.1 and $v_{\max}$=0.1 are chosen for the parameters τ and α and $v_{\min} = -0.1\bar{k}$, $v_{\max} = 0.1\bar{k}$ for the remaining model parameters. Taking into account the physical meaning of the parameter τ, the constraint τ>0 is modified to the following one 0<τ<1 without introducing any significant errors. If this constraint or the constraint 0<α<1 is violated then the appropriate element of the velocity vector $\mathbf{v}_j(k)$ is calculated from the formula (50) but with the first term omitted, and divided by 2.0. If the constrain is still violated, then the value of the objective function (44) is artificially multiplied by a number of the order 10^5. The objective function is also artificially multiplied when the constrains k_∞>0, k_0>0 or k>0 are not fulfilled. In the case of violation of the constrain k_∞>k_0, a new value of k_∞ equal to $1.01k_0$ is introduced.

5. Results of calculation

5.1 Results of typical calculation - the artificial data

A typical calculation is performed using artificially generated data. At the beginning, the artificial data without noises for all the considered models are calculated using formula (16) and assuming that: the number of excitation frequencies n=14; the parameters of the considered models are k_1=600.0 kN/m, k_2=400.0 kN/m, k=400.0 kN/m, c=150.0 kNs$^\alpha$/m, α=0.6 depending on the model which is considered and the following values of the dampers displacement amplitudes q_{si}=0.01 m, q_{ci}=0.005 m. The chosen values of the excitation frequency are taken from the range 0.5-13.5 Hz with the frequency increment $\Delta\lambda$=1.0 Hz. In our experiments we have used 20 particles. The maximum number of time instances was $i_{\max}$=400 and c_1=c_2=2.0. A size 3 neighbourhood was used as a trade-off between fast convergence and resistance to local minima. The PSO algorithm was applied 5 times with the final results presented in Table 1. It is evident that in the considered case and after using the presented identification method, the almost exact values of models parameters are obtained for all the considered models of dampers.

Moreover, the PSO procedure was applied to artificial data with artificially introduced noises. Random noises are added to the artificial data using the formulas

$$\begin{aligned} \hat{u}_{ci} &= (1+\tilde{r}_{1i}\varepsilon)\,\tilde{u}_{ci} \quad , \quad \hat{u}_{si} = (1+\tilde{r}_{2i}\varepsilon)\,\tilde{u}_{si} \quad , \\ \hat{q}_{ci} &= (1+\tilde{r}_{3i}\varepsilon)\,\tilde{q}_{ci} \quad , \quad \hat{q}_{si} = (1+\tilde{r}_{4i}\varepsilon)\,\tilde{q}_{si} \end{aligned} \tag{53}$$

where ε is the noise level, $\tilde{r}_{1i}$, $\tilde{r}_{2i}$, $\tilde{r}_{3i}$ and $\tilde{r}_{4i}$ are random numbers taken from the range from 0 to 1. The PSO algorithm was applied 20 times. Results of the calculation performed for different noise levels and different rheological models of dampers are presented in Table 2. Results presented in Table 2 indicate that the relative errors of values of α, k and c parameters are of the order of the noises introduced. The worst results are obtained for the Maxwell type four-parameter model which seems to be more sensitive to measurement errors than others.

In practice we are confronted with two kinds of errors. The first one is the measurements errors discussed above while the second one is the modelling errors. The modelling error occurs when the adopted rheological model of damper is, for example, to simple to be able to correctly describe all properties of the real VE damper. In order to illustrate the behaviours of the presented identification procedure we identify the parameters of one model on the basis of artificially generated data resulting from the other model. Firstly, the artificial data generated using the Kelvin type four-parameter model is approximated by the three-parameter Kelvin model. The obtained identification results are unacceptable. In the opposite case, i.e., when artificial data are generated for the three-parameter model and the four-parameter model is used in the identification procedure, the results are acceptable.

5.2 Results of typical calculation for real experimental data - viscoelastic damper

The identification procedure is also applied to identify parameters of liquid viscous damper investigated in papers by Makris (1992) and Makris and Constantinou (1991). The data given in paper by Makris (1992) are used to identify the parameters of all the considered rheological models.

In mentioned above papers dampers are modelled by the Maxwell type fractional rheological model described by the following equation

$$P_M(t) + \lambda_M D^r P_M(t) = C_{0M} D^q u_M(t) \tag{54}$$

where $P_M(t)$ denotes the damper force, $u_M(t)$ is now the damper displacement and λ_M, C_{0M}, r and q are the model parameters. The values of parameters of the above model identified by Makris (1992) are: λ_M=0.3$s^{0.6}$, C_{0M}=15.0 kNs/m, r=0.6, q=1.0. Please note that the above model has four parameters and is significantly different from the Maxwell type four-parameter model discussed in this paper and as described by Eq. (5). Except for the existence of two

Table 1 Results of identification procedure - artificial data without noises

Exact model parameters	k_1 $[kN/m]$	k_2 or k $[kN/m]$	c $[kNs^{\alpha}/m]$	α $[-]$
	600.0	400.0	150.0	0.6000
The three-parameter Kelvin model	-	399.6	150.1	0.5999
The three-parameter Maxwell model	-	400.0	150.0	0.6000
The Kelvin type four-parameter model	595.7	405.0	147.8	0.6094
The Maxwell type four-parameter model	599.9	400.3	150.4	0.5989

Table 2 Results of identification procedure - artificial data with noises

Exact model parameters		k_1 $[kN/m]$	k_2 or k $[kN/m]$	c $[kNs^{\alpha}/m]$	α $[-]$
		600.0	400.0	150.0	0.6000
The three-parameter Kelvin model	1.0%	-	390.5	152.8	0.5962
	2.0%	-	405.1	149.9	0.5999
The three-parameter Maxwell model	1.0%	-	398.2	150.6	0.6027
	2.0%	-	401.9	150.8	0.5962
The Kelvin type four-parameter model	1.0%	606.8	391.0	156.2	0.5815
	2.0%	596.5	404.3	151.4	0.6039
The Maxwell type four-parameter model	1.0%	590.9	412.3	165.7	0.5818
	2.0%	605.7	392.7	137.9	0.6101

Table 3 Results of identification procedure - data taken from Makris [1992]

Parameter	k_1 $[kN/m]$	k_2 or k $[kN/m]$	c $[kNs^{\alpha}/m]$	α $[-]$
Values of parameters taken from Makris	-	-	15.0 kNs/m	0.6000
The three-parameter Kelvin model	-	23.098	23.098	0.5110
The three-parameter Maxwell model	-	1402.79	20.663	0.5822
The Kelvin type four-parameter model	1196.2	0.5337	19.022	0.6049
The Maxwell type four-parameter model	0.04804	1364.19	20.402	0.5856

fractional derivatives of a different order, Eq. (54) exhibits some similarities with Eq. (21) which describes the dynamical behaviour of the three parameters Maxwell model.

The results obtained with the help of our identification procedure are presented in Table 3 and in Figs. 7-10 for all of the considered rheological models. In Fig. 7 the storage modulus versus excitation frequency is shown. The results obtained in the experiment are shown as small crosses and compared with the storage modulus obtained with the help of the three- and four-parameter Kelvin models. The results obtained from the three-parameter model are shown as the solid line with small rhombuses while the results obtained from the four-parameter model are shown as the solid line. In Fig. 8 the loss modulus is compared in a similar way. Figs. 9 and 10 give a comparison of experimental results with results obtained in the help of the three and four-parameter Maxwell models. Also in these figures, the results obtained from the three-parameter model are shown as the solid line with small rhombuses while the results obtained from the four-parameter model are shown as the solid line.

Some remarks can be formulated after a careful examination of the results, presented in Table 3 and Figs. 7-10.

- Parameter k_2 in the Kelvin type four-parameter model and the parameter k_1 of the Maxwell type four-parameter model are equal to zero in approximation.
- This means that for the considered liquid viscous damper the four-parameter models are essentially reduced to the three-parameter Maxwell model. The essential properties of the mentioned damper are incorporated in the three-parameters Maxwell model.
- However, a careful examination of the results presented in Figs. 7-10 suggests that the storage modulus and the loss modulus resulting from experiments are a little bit better approximated by the four-parameter models.
- In spite of some qualitative differences between Eqs. (54) and (21), the values of the fractional parameter and those of the damping factor of the two compared models are in good agreements where the liquid viscous damper parameters are identified.
- Despite the fact that the Maxwell models seems to be a better choice than the Kelvin models, the results obtained with the help of the Kelvin models can also be acceptable.

5.3 Results of typical calculation for real experimental data-viscoelastic fluids

Polydimethylsiloxane (C_2H_6OSi) is a highly viscous fluid, used in the experiments. Its rheological properties were investigated using the Physica MCR 101 dynamic shear rheometer. A system containing two parallel circular plates, 25 mm in diameter, was used in the experiments. The fluid was inserted in a 1.0 mm interstice between the plates. Its temperatures were 20°C and 50°C and were kept constant with a tolerance of ± 0.1 °C. The fluid was excited to a harmonic motion by rotating the movements of one plate. The amplitudes of angular motion were: 0.01 mrad; 1 mrad; 20 mrad and 100 mrad. For a given temperature and amplitude of motion, the experiments were performed for different excitation frequencies taken from the range 10^{-1}-10^{2} Hz. The storage modulus $E'(\lambda)$ and the loss modulus $E''(\lambda)$ were obtained from measurements.

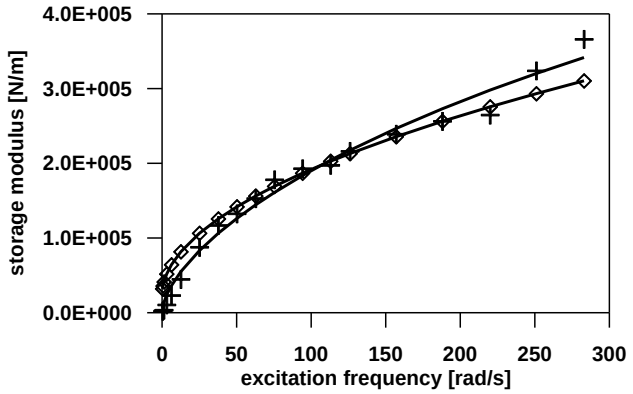

Fig. 7 Comparison of the experimentally obtained storage modulus (small crosses) with ones obtained using the three-parameter Kelvin model (solid line with rhombuses) and using the four-parameter Kelvin model (solid line)

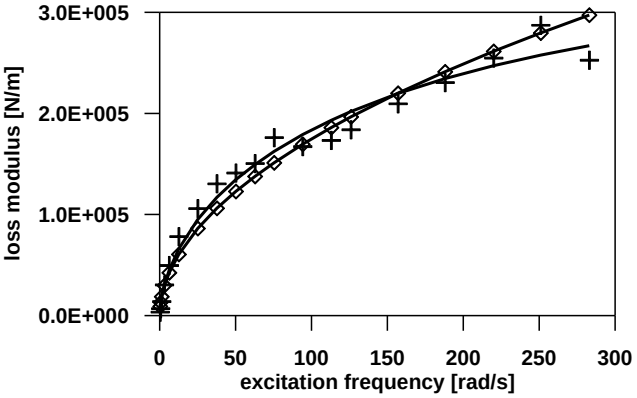

Fig. 8 Comparison of the experimentally obtained loss modulus (small crosses) with ones obtained using the three-parameter Kelvin model (solid line with rhombuses) and using the four-parameter Kelvin model (solid line

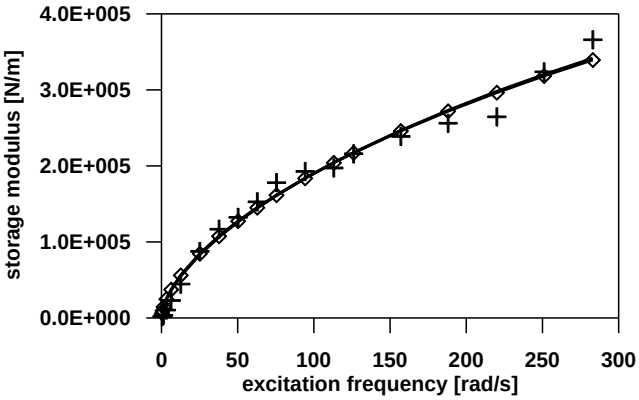

Fig. 9 Comparison of the experimentally obtained storage modulus (small crosses) with ones obtained using the three-parameter Maxwell model (solid line with rhombuses) and using the four-parameter Maxwell model (solid line)

Typical results obtained from the identification procedure are presented in Figs. 11 and 12. Moduli $E'(\lambda)$ and $E''(\lambda)$ are shown in relationship to the excitation

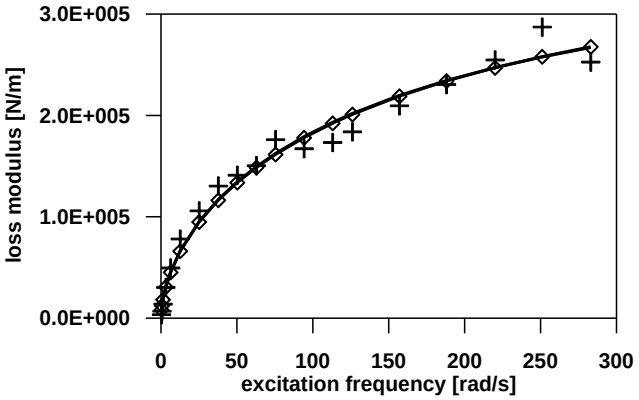

Fig. 10 Comparison of the experimentally obtained loss modulus (small crosses) with ones obtained using the three-parameter Maxwell model (solid line with rhombus) and using the four-parameter Maxwell model (solid line)

Table 4 Values of parameters of different models of fluids

Model	E or E_1 [Pa]	η or η_2 [Pa · s$^{\alpha}$]	E_2 [Pa]	α [-]
Maxwell	85931.0	2060.9	-	0.7500
Standard	92931.0	2129.4	0.0	0.7369
Zener	0.0	2067.8	88898.4	0.7301

Table 5 Dependence of parameter values on amplitudes of torsion vibration of rheometer

Amplitude [mrad]	Maxwell model			Standard model			
	E [Pa]	η [Pa·s$^{\alpha}$]	α [-]	E_1 [Pa]	E_2 [Pa]	η [Pa·s$^{\alpha}$]	α [-]
0.10	80614.7	2038.84	0.7544	80362.8	168.4	1999.2	0.7595
1.00	87876.0	2095.16	0.7470	96591.5	187.4	2172.0	0.7325
10.0	85931.0	2060.90	0.7500	92931.0	0.0	2129.4	0.7369

frequency λ. Results are for an amplitude of torsional motion equal to 10.0 mrad, the temperature during experiment was 20°C and the experimental data were taken from the range of 0.3-63.0 Hz.

The experimental data are shown by small crosses, while moduli resulting from identification procedure are presented by rhombi (Kelvin model), triangles (Maxwell model), squares (standard model) and by circles (Zener model). The results show that the properties of the investigated fluid cannot be described correctly by means of the three-parameter Kelvin model, therefore, the results obtained using this model will not be discussed in future. The values of parameters of the remaining models are presented in Table 4. The values of dynamic viscosity (η or η_2) in all the models are almost equal (differences are about 3%). Moreover, E_2=0 in the standard model and E_1=0 in the Zener model. This means that the four-parameter models are reduced to the three-parameter Maxwell model. Differences between the values of E are about 8% while differences in the values of the parameter α (the order of fractional derivative) are not greater than 3%. All of this

justifies the effectiveness of the proposed method of identification.

In Table 5, the values of parameters of the Maxwell model and the standard model are presented for three different amplitudes of torsional vibration of rheometer. In the considered range of amplitudes, the values of model parameters are approximately constant.

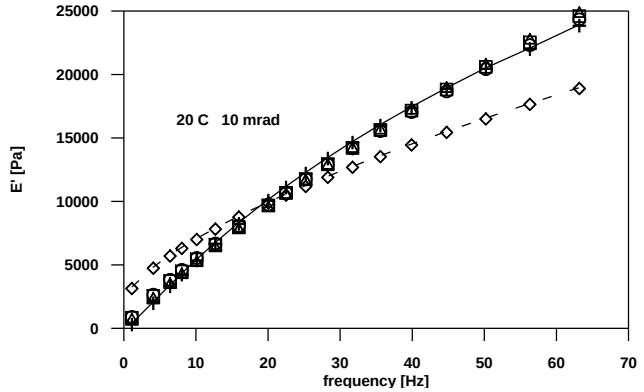

Fig. 11 Comparison of identification results - modulus E' vs. excitation frequency, experimental results (+), Kelvin model (✂), Maxwell model (🖻), standard model ( ), Zener model (○)

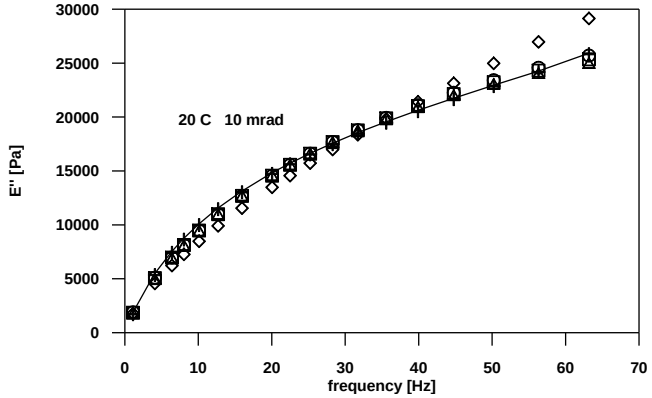

Fig. 12 Comparison of identification results – modulus E'' vs. excitation frequency, experimental results (+), Kelvin model (✂), Maxwell model (🖻), standard model ( ), Zener model (○)

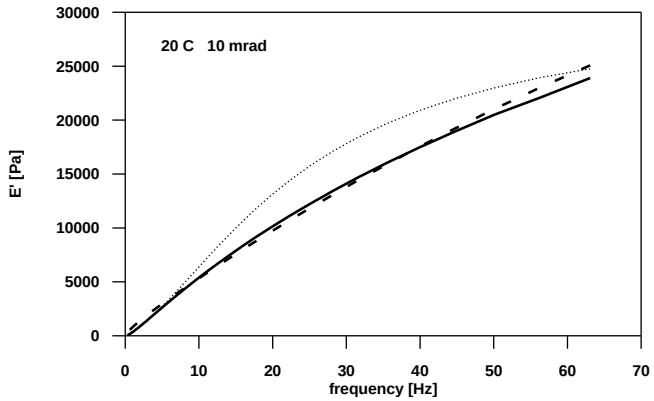

Fig. 13 Course of function $E'(\lambda)$ for different values of parameters of the Maxwell model

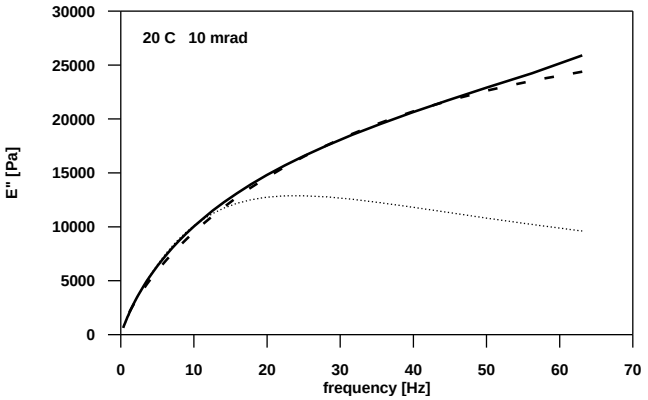

Fig. 14 Course of function $E''(\lambda)$ for different values of parameters of the Maxwell model

Table 6 Dependence of parameter values on a range of excitation frequencies

Number of data	Range of frequencies [Hz]	Maxwell model		
		E [Pa]	η [Pa·s$^{\alpha}$]	α [-]
1	0.3-63.0	80614.7	2038.8	0.7544
2	0.3-50.0	75925.2	1992.2	0.7676
3	0.3-43.0	68786.9	1941.9	0.8009
4	0.3-28.0	60248.8	1885.1	0.8033
5	0.3-20.0	52960.2	1843.2	0.8229
6	0.3-10.0	40452.7	1793.3	0.8602
7	0.3-5.0	30474.4	1781.8	0.8937

In Table 6, the influence of a range of experimental data on the results of identification of model parameters is presented for the Maxwell model. The observed influence is highly significant. The values of the parameters E and η considerably decrease with an increase in the range of excitation frequencies while the values of the parameter α increase. The maximum differences are: 62.1% for E, 12.6% for η and 18.5% for α. Figs. 13 and 14 illustrate how these effects influence the storage modulus and the loss modulus, respectively. In the figures, the solid line shows a modulus obtained from the experimental data while the dashed line and the dotted line are obtained when parameters from the first and the last line of Table 6 are used, respectively. Differences in predicting the loss modulus are not only quantitative but also qualitative because function $E''(\lambda)$ has its minimum when data from the last line of Table 6 are used. Such results seem to indicate that the results of identification are valid approximately only in a range of frequencies for which the experimental data are available.

Partial explanation of the inability to correctly predict the modules $E'(\lambda)$ and $E''(\lambda)$ outside the range of available experimental data is feasible on the basis of sensitivity analysis. The formulae for the needed sensitivities $\partial E'(\lambda)/\partial E$, $\partial E'(\lambda)/\partial \eta$, $\partial E'(\lambda)/\partial \alpha$, $\partial E''(\lambda)/\partial E$, $\partial E''(\lambda)/\partial \eta$ and $\partial E''(\lambda)/\partial \varepsilon$ have been obtained performing symbolic differentiations with the help of

MATLAB. It is easy to conclude that such sensitivities depend on the current values of the model parameters (E, η and α) and the excitation frequency λ. Only the sensitivities $\partial E''(\lambda)/\partial E$, $\partial E''(\lambda)/\partial \eta$ and $\partial E''(\lambda)/\partial \varepsilon$, treated as functions of λ, are presented in Figs. 15-17. These functions are shown for different values of model parameters taken from Table 6 and the diagrams are numbered as the corresponding model parameters in Table 6. The shapes of the functions are highly various. In all the figures, it can be seen that, for low frequencies, the values of sensitivity functions are very similar and have significantly or completely different values for high frequencies. The region where sensitivities are similar is strongly related to the range of frequencies from which the experimental data are taken. For a larger range of experimental data, we can see a larger range of excitation frequencies where values of sensitivities are similar. For small ranges of experimental data, the different values of sensitivity functions are completely different, in comparison with the corresponding values of sensitivity functions obtained for the large ranges of experimental data. Similar conclusions result from the analysis of sensitivities $\partial E'(\lambda)/\partial E$, $\partial E'(\lambda)/\partial \eta$ and $\partial E'(\lambda)/\partial \alpha$.

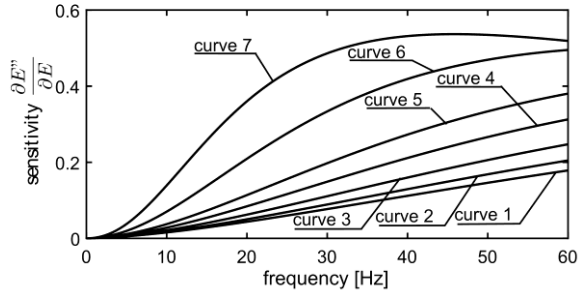

Fig. 15 Sensitivites $\partial E''(\lambda)/\partial E$ for different values of parameters of the Maxwell model

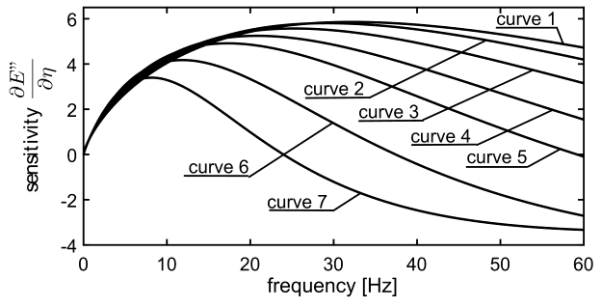

Fig. 16 Sensitivites $\partial E''(\lambda)/\partial \eta$ for different values of parameters of the Maxwell model

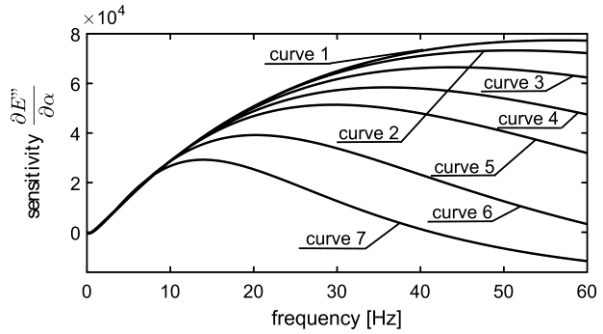

Fig. 17 Sensitivites $\partial E''(\lambda)/\partial \alpha$ for different values of parameters of the Maxwell model

6. Conclusions

The proposed identification method can be used effectively for determining the parameters of a group of rheological models with fractional derivatives. Its effectiveness has successfully been tested using both artificial data and data for a real damper taken from literature, as well as the authors' own data concerning a highly viscous fluid. The data taken from the dynamical experiments are used to identify the parameters of the rheological models. The identification procedure proposed in this paper seems to be quite general and applicable to determination of the parameters of other rheological models with fractional derivatives. The above-mentioned rheological models can be used to modelling the dynamic behaviour of VE dampers and highly viscous fluids. The identification problem is reduced to the nonlinear optimization problem which is solved by means of the particle swarm optimization method. Based on calculation presented in this paper for the artificially generated data, it was found that the proposed method is not sensitive to noises introduced during the measurements.

Acknowledgments

This study is supported by the National Science Centre, Poland, as part of Project No. DEC/2013/09/B/ST8/01733, carried out in the years 2014-2017. This support is gratefully acknowledged.

References

Aprile, A, Inaudi, J.A. and Kelly, J.M. (1997), "Evolutionary model of viscoelastic dampers for structural applications", *J. Eng. Mech.*, **123**(6), 551-560.

Bagley, R.L. and Torvik, P.J. (1989), "Fractional calculus-a different approach to the analysis of viscoelastically damped structures", *AIAA J.*, **27**, 1412-1417.

Bucher, C. and Pirrotta, A. (2015), "Dynamic finite element analysis of fractionally damped structural systems in the time domain", *Acta Mech.*, **226**(12), 3977-3990.

Chang, T. and Singh, M.P. (2002), "Seismic analysis of structures with a fractional derivative model of viscoelastic dampers", *Earthq. Eng. Eng. Vib.*, **1**(2), 251-260.

Chang, T.S. and Singh, M.P. (2009), "Mechanical model parameters for viscoelastic dampers", *J. Eng. Mech.*, **135**(6), 581-584.

Christopoulos, C and Filiatrault, A. (2006), *Principles of passive supplemental damping and seismic isolation*, IUSS Press, Pavia, Italy.

Cortés, F. and Elejabarrieta, M.J. (2007), "Finite element formulations for transient dynamic analysis in structural

systems with viscoelastic treatments containing fractional derivative models", *Int. J. Num. Meth. Eng.*, **69**(10), 2173-219.

Couceiro, M. and Ghamisi, P. (2016), *Fractional order darwinian particle swarm optimization Applications and evaluation of an evolutionary algorithm*, Springer, Heidelberg New York, Dordrecht, London

Di Paola, M., Pirrotta, A. and Valenza, A. (2011), "Visco-elastic behavior through fractional calculus: An easier method for best fitting experimental results", *Mech. Mater*., **43**(12), 799-808.

Enelund, M. and Olsson, P. (1999), "Damping described by fading memory analysis and application to fractional derivative models", *Int. J. Solids Struct.*, **36**(7), 939-970.

Fan, W., Jiang, X. and Qi, H. (2015), "Parameter estimation for the generalized fractional element network Zener model based on the Bayesian method", *Physica A*, **427**, 40-49.

Fenander, A. (1996), "Modal synthesis when modeling damping by use of fractional derivatives", *AIAA J*., **34**(5), 1051-1058.

Frings, C. and De La Llera, J.C. (2011), "Multiphysics modeling and experimental behavior of viscous damper", eds., G. De Roeck, G. Degrande, G. Lambert, G. Muller, *The 8th International Conference on Structural Dynamics, (EURODYN 2011)*, Leuven, Belgium, July 4-6.

Galucio, A.C., Deu, J.F. and Ohayon, R. (2004), "Finite element formulation of viscoelastic sandwich beams using fractional derivative operators", *Comp. Mech.*, **33**(4), 282-291.

Gerlach, S. and Matzenmiller, A. (2005), "Comparison of numerical methods for identification of viscoelastic line spectra from static test data", *Int. J. Num. Meth. Eng.*, **63**(3), 428-454.

Greco, R., Avakian, J. and Marano, G.C. (2014), "A comparative study on parametr identification of fluid viscous pampers with different models", *Arch. Appl. Mech*., **84**, 117-1134.

Gupta, N., Machida, A., Mutsyoshi, H. and Tanzo, W. (1996), "A fractional derivative hysteretic model for viscoelastic damper", *J. Struct. Eng.*, **42**, 697-706.

Gusella, V. and Terenzi, G. (1997), "Fluid viscous device modeling by fractional derivatives", *Struct. Eng. Mech.*, **5**(2), 177-191.

Hansen, S. (2007), "Estimation of the relaxation spectrum from dynamic experiments using Bayesian analysis and a new regularization constraint", *Rheol. Acta*, **47**(2), 169-178.

Hatada, T., Kobori, T., Ishida, M. and Niwa, N. (2000), "Dynamic analysis of structures with Maxwell model", *Earthq. Eng. Struct. D.*, **29**(2), 159-176.

Hayat, T., Nadeem, S. and Asghar, S. (2004), "Periodic unidirectional flows of a viscoelastic fluid with the fractional Maxwell model", *Appl.Math. Comp*., **151**(1), 153-161.

Hou, C.Y. (2008), "Fluids dynamics and behavior of nonlinear fluid dampers", *J. Struct. Eng*., **134**, 56-63.

Idesman, A., Niekamp, R. and Stein, E. (2001), "Finite elements in space and time for generalized viscoelastic model", *Comput. Mech.*, **27**(1), 49-60.

Jones, D.I.G. (2001), *Handbook of viscoelastic vibration damping*. Wiley, New York, USA.

Kennedy, J. and Eberhart, R.C. (1995), "Particle swarm optimization", *IEEE International Conference on Neural Networks*, **4**, 1942-1948.

Khan, M., Anjum, A., Qi, H. and Fetecau, C. (2010), "On exact solutions for some oscillating motions of a generalized Oldroyd-B fluid", *Zeitschrift für Angewandte Mathematik und Physik*, **61**(1), 133-145.

Lee, S.H., Son, D.I., Kim, J. and Min, K.W. (2004), "Optimal design of viscoelastic dampers using eigenvalue assignment", *Earthq. Eng. Struct. D.*, **33**(4), 521-542.

Lewandowski, R. and Chorążyczewski, B. (2010), "Identification of the parameters of the Kelvin-Voigt and the Maxwell fractional models, used to modeling of viscoelastic dampers", *Comp. Struct.*, **88**(1), 1-17.

Lewandowski, R., Bartkowiak, A. and Maciejewski H. (2012), "Dynamic analysis of frames with viscoelastic dampers: a comparison of damper models", *Struct. Eng. Mech.*, **41**(1), 113-137.

Lewandowski, R. and Pawlak, Z. (2011), "Dynamic analysis of frames with viscoelastic dampers modelled by rheological models with fractional derivatives", *J. Sound Vib*., **330**(5), 923-936.

Lion, A. (2001), "Thermomechanically consistent formulations of the standard linear solid using fractional derivatives", *Arch. Mech.*, **53**(3), 253-273.

Makris, N. (1992), *Theoretical and experimental investigation of viscous dampers in applications of seismic and vibration isolation*, PhD dissertation, State University of New York at Buffalo.

Makris, N. and Constantinou, M.C. (1991), "Fractional-derivative Maxwell model for viscous dampers", *J. Struct. Eng.*, ASCE, **117**(9), 2708-2724.

Matsagar, V.A. and Jangid, R.S. (2005), "Viscoelastic damper connected to adjacent structures involving seismic isolation", *J. Civ. Eng. Manage.*, **11**(4), 309-322.

Okada, R., Nakata, N., Spencer, B.F., Kasai, K. and Kim, B.S. (2006), "Rational polynomial approximation modeling for analysis of structures with VE dampers", *J. Earthq. Eng*., **10**(1), 97-125.

Palmeri, A., Ricciardelli, F., De Luca, A. and Muscolino, G. (2003), "State space formulation for linear viscoelastic dynamic systems with memory", *J. Eng. Mech.*, **129**(7), 715-724.

Park, S.W. (2001), "Analytical modeling of viscoelastic dampers for structural and vibration control", *Int. J. Solids Struct.*, **38**(44), 8065-8092.

Park, J.H., Kim, J. and Min, K.W. (2004), "Optimal design of added viscoelastic dampers and supporting braces", *Earthq. Eng. Struct. D.*, **33**(4), 465-484.

Perez, R.E. and Behdinan, K. (2007), "Particle swarm approach for structural design optimization", *Comp. Struct.*, **85**(19), 1579-1588.

Pirrotta, A., Cutrona, S., Di Lorenzo, S. and Di Mateo, A. (2015), "Fractional visco-elastic Timoshenko beam deflection via single equation", *Int. J. Numer. Meth. Eng*., **104**(9), 869-886.

Podlubny, I. (1999), *Fractional differential equations*, Academic Press, New York, USA.

Pritz, T. (1996), "Analysis of four-parameter fractional derivative model of real solid materials", *J. Sound Vib.*, **195**(1), 103-115.

Pritz, T. (2003), "Five-parameter fractional derivative model for polymeric damping materials", *J. Sound Vib.*, **265**(5), 935-952.

Schmidt, A. and Gaul, L. (2002), "Finite element formulation of viscoelastic constitutive equations using fractional time derivatives", *J. Nonlin. Dyn.*, **29**(1), 37-55.

Shukla, A.K. and Datta, T.K. (1999), "Optimal use of viscoelastic dampers in building frames for seismic force", *J. Struct. Eng.*, **125**(4), 401-409.

Singh, M.P. and Chang, T.S. (2009), "Seismic analysis of structures with viscoelastic dampers", *J. Eng. Mech.*, **135**(6), 571-580.

Singh, M.P. and Moreschi, L.M. (2002), "Optimal placement of dampers for passive response control", *Earthq. Eng. Struct. D.*, **31**(4), 955-976.

Singh, M.P., Verma, N.P. and Moreschi, L.M. (2003), "Seismic analysis and design with Maxwell dampers", *J. Eng. Mech.*, **129**(3), 273-282.

Tong, D. and Liu, Y. (2005), "Exact solutions for the unsteady rotational flow of non-Newtonian fluid in an annular pipe", *Int. J. Eng. Sci.*, **43**(3), 281-289.

Tsai, M.H. and Chang, K.C. (2002), "Higher-mode effect on the seismic responses of buildings with viscoelastic dampers", *Earthq. Eng. Eng. Vib*., **1**(1), 119-129.

Yang, P., Lam, Y. and Zhu, K. (2010), "Constitutive equation with fractional derivatives for the generalized UCM model", *J. Non-Newtonian Fluid Mech*., **165**(3), 88-97.

Yin, Y. and Zhu, K.Q. (2006), "Oscillating flow of a viscoelastic fluid in a pipe with the fractional Maxwell mode", *Appl. Math. Comp*., **173**(1), 231-242.

Welch, S.W.J., Rorrer, R.A.L. and Duren, R.G. (1999), "Application of time-based fractional calculus methods to viscoelastic creep and stress relaxation of materials", *Mech. Time-Dependent Mater.*, **3**(3), 279-303.

Wilke, D.N., Kok, S. and Groenwold, A.A. (2007), "Comparison of linear and classical velocity update rules in particle swarm optimization: Notes on diversity", *Int. J. Num. Meth. Eng.*, **70**(8), 962-984.

Xu, H. and Jiang, X. (2016), "Creep constitutive models for viscoelastic materials based on fractional derivatives", *Comp. Math. Appl*., **73**(6), 1377-1384.

CC